Trans. Japan Soc. Aero. Space Sci.
Vol. 56, No. 3, pp. 170–172, 2013

Research Note

Analysis of Laser Wavelength and Energy Dependences of the Impulse in a Magnetic Thrust Chamber System for a Laser Fusion Rocket

By Akihiro MAENO,[1)] Naoji YAMAMOTO,[1)] Shinsuke FUJIOKA,[2)] Yoshitaka MORI,[3)] Atsushi SUNAHARA,[4)] Tomoyuki JOHZAKI[5)] and Hideki NAKASHIMA[1)]

[1)]*Interdisciplinary Graduate School of Engineering Science, Kyushu University, Kasuga, Japan*
[2)]*Institute of Laser Engineering, Osaka University, Suita, Japan*
[3)]*The Graduate School for the Creation of New Photonics Industries, Hamamatsu, Japan*
[4)]*Institute for Laser Technology, Suita, Japan*
[5)]*Graduate School of Engineering, Hiroshima University, Higashi-Hiroshima, Japan*

(Received March 22nd, 2012)

Experiments using a pendulum thrust stand are performed to determine the dependences of the impulse on the laser wavelength and energy in a magnetic thrust chamber system for a laser fusion rocket. The impulse is generated by the interaction between a diamagnetic current in a laser-produced plasma and a magnetic field. The plasma is produced by irradiating a spherical polyacetal target with a single-beam glass laser (laser pulse duration: 1.3 ns; laser wavelengths: 1,053, 527 and 351 nm; laser energy: 30–900 J). The magnetic field is generated by a cylindrical neodymium permanent magnet (50 mm diameter and 40 mm long) placed in a position 33 mm from the target. Impulses in the range 0.02–10 mNs are measured using a pendulum thrust stand. The experiments reveal that the impulse for 2ω is similar to that for 3ω, and is larger than that for ω.

Key Words: Propulsion, Laser-Produced Plasma, Magnetic Thrust Chamber System, Laser Fusion Rocket

Laser fusion rockets (LFR)[1)] that generate large thrust and high specific impulse will be necessary for manned space flights to Mars. This rocket employs a magnetic thrust chamber system, which produces an impulse due to the interaction between a diamagnetic current in a laser-produced plasma and a magnetic field. The system of an LFR consists of inertial confinement fusion (ICF) plasma and the magnetic field geometry produced by a solenoid superconducting magnet (SCM). In these experiments, a laser-produced plasma and a neodymium permanent magnet are used instead of ICF plasma and SCM. Figure 1 depicts the mechanism for producing an impulse.

Several experiments have investigated the plasma behaviors in a magnetic field. Vchivokv et al.[2)] observed temporal plasma behaviors in an axially symmetric dipole magnetic field. Using a magnetic probe, they found that a diamagnetic cavity forms in the applied magnetic field. Our research group[3)] has experimentally demonstrated the system for an LFR by measuring the impulse using a pendulum thrust stand. When a magnetic field is not applied, there is no measurable impulse. This result indicates that the system is capable of generating impulses. It is also found that the impulse increases with increasing laser pulse duration. In this paper, we experimentally investigate the dependences of the impulse on the laser wavelength and energy.

In these experiments, the impulse is measured using a pendulum thrust stand (see Fig. 2). A plasma is generated by focusing a 1.3 ns laser pulse onto a 1.5 mm diameter spherical polyacetal target at the GEKKO XII facility, Osaka University. The laser beam is focused using a lens (F-number: 3) so that its diameter is equal to that of the target. The target is suspended at the end of a carbon fiber attached to a glass rod to reduce the measurement error caused by the ablation plasma generated by the glass rod. A cylindrical neodymium permanent magnet was used to generate the magnetic field. The maximum energy product of the magnet is 0.382 mJ/mm^3. The magnet is 50 mm diameter and 40 mm long. It is positioned so that it does not obstruct the incident laser beam. The distance between the magnet surface and the target center is 33 mm and the angle between the magnet axis and the laser beam is 66.5°. The magnetic field strength at the target is calculated to be 0.1 T, as shown in Fig. 3.

The pendulum thrust stand[4)] consists of a magnet, bearings, a counterweight and light emitting diode (LED) displacement sensors. The magnet is installed on top of the pendulum. The pendulum is supported by the bearings, which are mounted on side posts. The counterweight is placed on the pendulum such that the center of gravity lies in the pendulum's axis of rotation. This ensures that the pendulum swings easily even for a small impulse. The pendulum has a natural period of 1.3 s. This is short enough to reduce the mechanical noise induced by background vibrations, which are problematic when measuring small impulses. The LED displacement sensors detect the deflection of the pendulum. To eliminate momentum transfer due to direct collisions between the expanding plasma and the magnet, a plate connected to a grounded vacuum chamber is placed 2 mm from the magnet to shield it from the plasma.

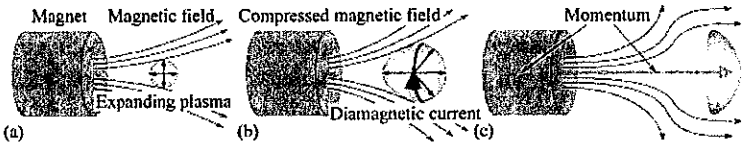

Fig. 1. Mechanism for producing an impulse in a magnetic thrust chamber system for an LFR.
(a) Expanding a laser-produced plasma in a magnetic field geometry generated by a neodymium permanent magnet. (b) Compressed magnetic field and diamagnetic current induced by Larmor motion. (c) Compressed magnetic field pushing back the plasma.

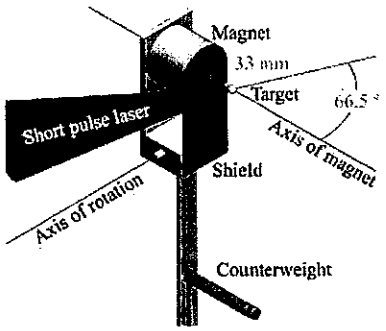

Fig. 2. Experimental setup and schematic drawing of the pendulum thrust stand.

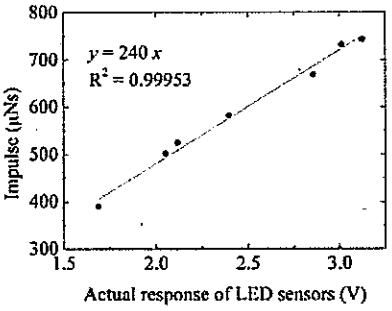

Fig. 4. Applied calibration force as a function of the LED sensor signals; the line is the best fit to the calibration data.

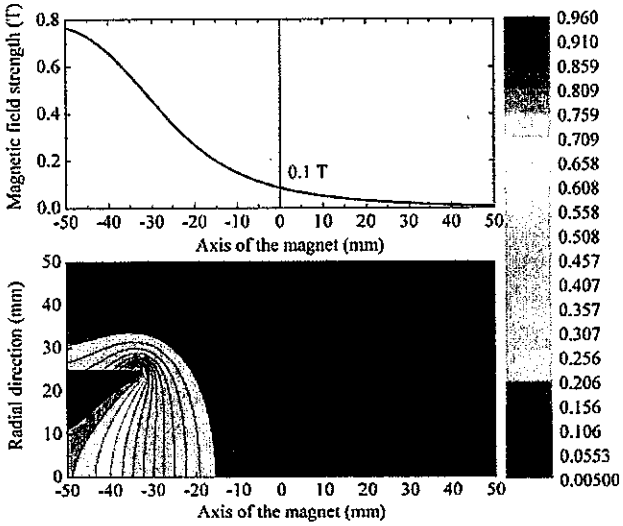

Fig. 3. Calculated magnetic field strength along the axis of the magnet and on the plane when the target is set on the center.
The magnetic field strength at the center is 0.1 T.

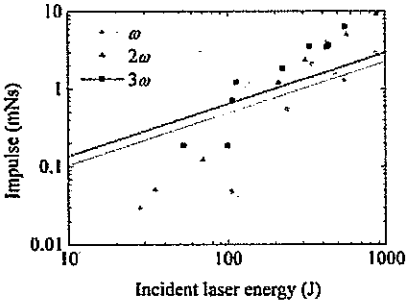

Fig. 5. Impulses measured by the thrust stand as a function of incident laser energy for laser frequencies of ω, 2ω and 3ω.

The thrust stand is calibrated by striking the thrust stand to cause an impact. The impact is directly measured by a force transducer attached to the counterweight. The force transducer records the impulsive force as a function of time; integrating this yields the applied impulse. It is assumed that the impulse on the force transducer is proportional to the amplitude of the output of the LED displacement sensors, which measure the deflection of the pendulum. Based on this assumption, we linearly fit the calibration data, as shown in Fig. 4. The R^2 coefficient is 0.99953. The experimental data are converted into forces using a conversion factor of 240 μNs/V, which is obtained from the calibration. The detection limit of the thrust stand is found to be 17 μNs.

Figure 5 shows the impulses measured on the thrust stand as a function of the incident laser energy. The three data sets show impulses for single laser pulses with frequencies of ω ($\lambda = 1{,}053$ nm), 2ω ($\lambda = 527$ nm) and 3ω ($\lambda = 351$ nm), where λ is the laser wavelength. Impulses of 1.3, 5.0, and 6.4 mNs are generated at laser frequencies of ω, 2ω and 3ω for incident laser energies of 548, 568 and 550 J, respectively. Figure 5 shows that 2ω produces similar impulses as 3ω and that they both produce larger impulses than ω. In addition, it shows that the impulse increases with increasing incident laser energy.

The impulse for a specific laser wavelength is estimated using a theoretical model. The lines in Fig. 5 are the estimated impulse curves obtained by assuming that the impulse is equal to the product of the plasma ablation mass and the ion acoustic speed (i.e., $S\tau\dot{m}C_s$) and that all the plasma is pushed back by the magnetic field before it col-

lides with the plate of thrust stand. S is the plasma ablation area of the target, which is assumed to be equal to the target surface for a solid angle of 2π since the target is irradiated by a single laser beam through a lens with an F-number of 3. Thus, S is constant at $3.5 \times 10^{-6}\,\mathrm{m}^2$. The laser pulse duration τ is 1.3 ns. The expansion velocity of the plasma into vacuum is approximately equal to the ion acoustic speed. The plasma ablation mass per unit area per unit time $\dot{m}$ and the ion acoustic speed C_s are calculated as follows. Equation (1) gives $\dot{m}$, where m_e and m_i are the electron and ion masses, respectively. The charge number of the ions Z is four since C^{4+} is assumed to be the primary ion in the plasma, the laser absorption rate η_a is assumed to be one, and the coefficient f is 0.08. I is the incident laser intensity, which follows the relation $I = E_L/S\tau$, where E_L is the incident laser energy. Equation (2) gives C_s. n_c is the laser critical density, which follows the relation $n_c = 4\pi m_e/\mu_0 e^2\lambda^2$, where μ_0 is the permeability of vacuum and e is the elementary electric charge. In this case, the laser critical density for each laser frequency is $1.0 \times 10^{27}\,\mathrm{m}^{-3}$ for ω, $4.0 \times 10^{27}\,\mathrm{m}^{-3}$ for 2ω, and $9.0 \times 10^{27}\,\mathrm{m}^{-3}$ for 3ω. According to these equations, the product of the plasma ablation mass and the expansion velocity increases with increasing laser critical density and incident laser energy; that is, $\dot{m}C_s \propto \lambda^{-2/3}$ and $I^{2/3}$. When E_L is constant, the impulse is proportional to $S\tau\dot{m}C_s \propto \lambda^{-2/3}$ and $I^{2/3}$. Thus, the estimated impulse increases with decreasing laser wavelength and increasing incident laser energy. The measured impulses, which are indicated by the plots in Fig. 5, exhibit the same trends as the theoretical model.

$$\dot{m} = \frac{n_c^{2/3}}{Z}\left(\frac{3\eta_a I}{4f}\right)^{1/3}\sqrt{(1+Z)m_e^{1/3}m_i} \tag{1}$$

$$C_s = \left(\frac{3\eta_a I}{4fn_c}\right)^{1/3}\sqrt{\frac{(1+Z)m_e^{1/3}}{m_i}} \tag{2}$$

In the present experiments, the laser wavelength and energy dependences of the impulse were investigated to optimize the magnetic thrust chamber system for an LFR for various experimental conditions. The impulse as a function of incident laser energy for 2ω was found to be similar to that for 3ω but larger than that for ω. Thus, the relationship between the measured impulse and the laser wavelength was determined. This can be explained theoretically by values expressed in terms of the product of the plasma ablation mass and the ion acoustic speed. As a result, for producing large impulse, it was found that longer pulse durations, shorter wavelengths and higher energies are better.

Acknowledgments

The authors wish to thank the Grant-in-Aid for Scientific Research (B), No. 21360418, and the Grant-in-Aid for JSPS Fellows sponsored by the Japan Society for the Promotion of Science, No. 22-1672, Japan. This work was performed under Collaborative Research, Institute of Laser Engineering, Osaka University, No. A1-01, 2009.

References

1) Hyde, R. A., Wood, L. L. and Nuckolls, J. H.: Prospects for Rocket Propulsion with Laser-Induced Fusion Microexplosions, AIAA Paper 72-1063, 1972.
2) Vchivokv, K. V., Nakashima, H., Zakharov, Y. P., Esaki, T., Kawano, T. and Muranaka, T.: Laser-Produced Plasma Experiments and Particle in Cell Simulation to Study Thrust Conversion Processes in a Laser Fusion Rocket, *Jpn. J. Appl. Phys.*, **42** (2003), pp. 6590–6597.
3) Maeno, A., Yamamoto, N., Nakashima, H., Fujioka, S., Mori, Y., Sunahara, A. and Johzaki, T.: Direct Measurement of the Impulse in a Magnetic Thrust Chamber System for Laser Fusion Rocket, *Appl. Phys. Lett.*, **99** (2011), 071501.
4) Koizumi, K., Komurasaki, K. and Arakawa, Y.: Development of Thrust Stand for Low Impulse Measurement from Microthrusters, *Rev. Sci. Instrum*, **75** (2004), pp. 3185–3189.